ACS OMEGA

Article

http://pubs.acs.org/journal/acsodf

# Microwave Heating of Synthetic Skin Samples for Potential Treatment of Gout Using the Metal-Assisted and Microwave-Accelerated Decrystallization Technique

Salih Toker,[†] Zainab Boone-Kukoyi,[†] Nishone Thompson,[†] Hillary Ajifa,[†] Travis Clement,[†] Birol Ozturk,[‡] and Kadir Aslan*[,†]

[†]Department of Chemistry and [‡]Department of Physics and Engineering Physics, Morgan State University, 1700 East Cold Spring Lane, Baltimore, Maryland 21251, United States

Supporting Information

**ABSTRACT:** Physical stability of synthetic skin samples during their exposure to microwave heating was investigated to demonstrate the use of the metal-assisted and microwave-accelerated decrystallization (MAMAD) technique for potential biomedical applications. In this regard, optical microscopy and temperature measurements were employed for the qualitative and quantitative assessment of damage to synthetic skin samples during 20 s intermittent microwave heating using a monomode microwave source (at 8 GHz, 2−20 W) up to 120 s. The extent of damage to synthetic skin samples, assessed by the change in the surface area of skin samples, was negligible for microwave power of ≤7 W and more extensive damage (>50%) to skin samples occurred when exposed to >7 W at initial temperature range of 20−39 °C. The initial temperature of synthetic skin samples significantly affected the extent of change in temperature of synthetic skin samples during their exposure to microwave heating. The proof of principle use of the MAMAD technique was demonstrated for the decrystallization of a model biological crystal (L-alanine) placed under synthetic skin samples in the presence of gold nanoparticles. Our results showed that the size (initial size ∼850 μm) of L-alanine crystals can be reduced up to 60% in 120 s without damage to synthetic skin samples using the MAMAD technique. Finite-difference time-domain-based simulations of the electric field distribution of an 8 GHz monomode microwave radiation showed that synthetic skin samples are predicted to absorb ∼92.2% of the microwave radiation.

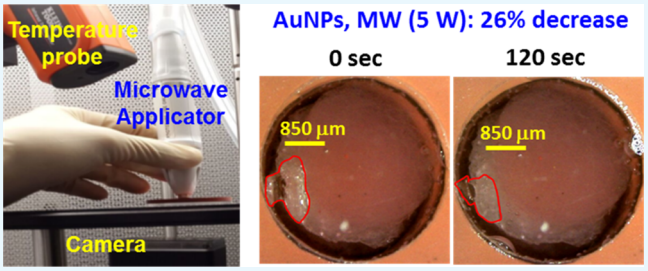


## INTRODUCTION

Hyperuricemia, a precursor for gout disease, is caused by elevated serum levels of uric acid and results in the buildup of monosodium urate monohydrate (MSUM) crystals in the soft tissue of humans. Normal serum uric acid levels range from 3.5 to 7.2 mg/dL. Consistent levels above the normal range result in acute gout, which gradually advances into chronic gout.[1−5] Chronic gout arises when MSUM crystals accumulate in the synovial joints and the surrounding soft tissues to subsequently form aggregates, also known as tophi.[6] Current therapies for gout include the systematic use of nonsteroidal anti-inflammatory drugs (NSAIDs) as chemical therapeutics for inflammation and uricosuria agents for the reduction of uric acid reuptake by the kidneys.[7,8] NSAIDs and uricosuria agents have numerous systemic side effects, such as stomach ulcers, decubitus ulcers, osteoporosis, and decreased function of the immune system.[9,10] For extreme cases of chronic gout, surgery is often recommended for the removal of tophi masses.[11,12] The breach of the main barrier (skin tissue) during invasive surgical removal of crystal aggregates often poses a major risk of infection to the joints, destroying joints, resulting in a need for amputation.[13,14] Consequently, there is still a need for alternative noninvasive therapies for the treatment of gout.

Microwaves have been used as therapeutic and diagnostic aids in the field of medicine and surgery.[15,16] The use of microwaves in other aspects of biomedicine, such as in hyperthermia therapy, inflammation therapy, and in the diagnosis and treatment of cancer, is also on the rise.[15−17] The efficiency of microwave heating of tissue samples depends on the frequency of the microwaves and the penetration depth of the waves through dielectric materials within the skin.[16,17] In this regard, microwaves with lower frequency can penetrate deeper into the skin than the microwaves with higher frequency.[18,19] For example, microwave systems operating at 915 MHz and 2.45 GHz are suited for large volume ablation,[17] whereas the use of higher frequencies is suitable for treatments such as skin cancer, ablation of heart tissue to treat arrhythmia, uterine fibroids, multiple small liver metastases, corneal ablation for vision correction, spinal nerve ablation to treat back pain,

Received: September 8, 2016
Accepted: October 17, 2016
Published: November 1, 2016

  

DOI: 10.1021/acsomega.6b00233
ACS Omega 2016, 1, 744−754

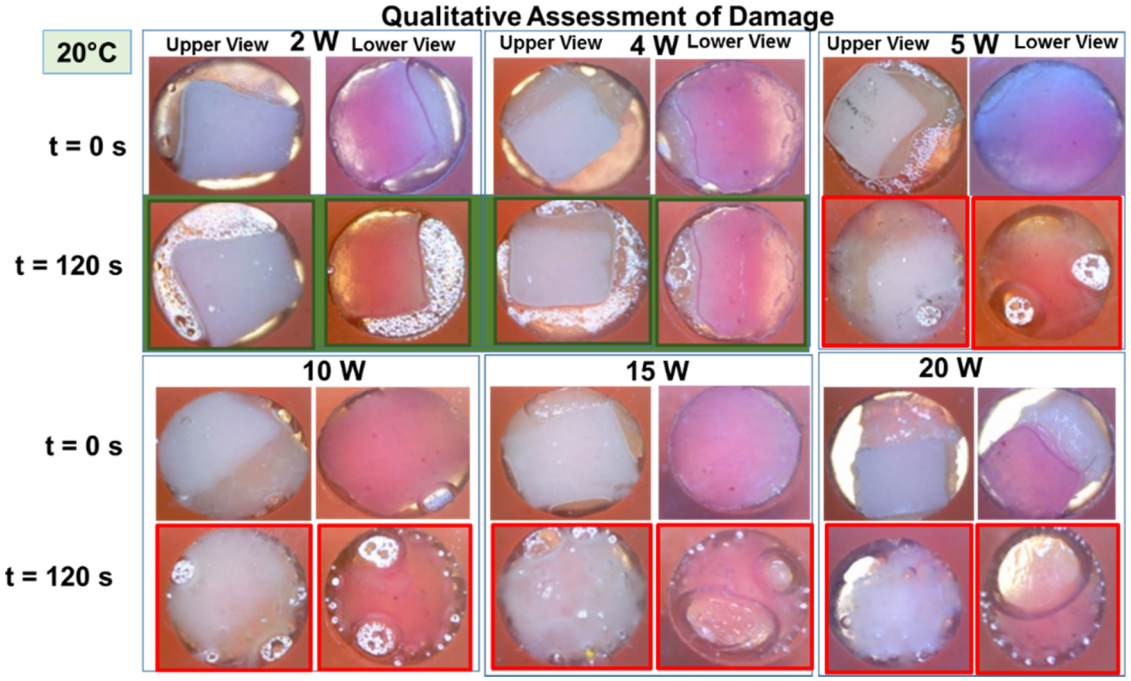


**Figure 1.** Qualitative assessment of skin damage via visual confirmation. Real-color pictures of synthetic skin samples at an initial temperature of 20 °C before and after their exposure to 20 s intervals of microwave heating at 2, 4, 5, 10, 15, and 20 W up to 120 s. Green frames denote no tissue damage at 2 and 4 W. Red frames denote tissue damage after 120 s of microwave heating at 5, 10, 15, and 20 W.

varicose vein treatment, and verrucae treatment. Higher frequency treatments in the range 5.8−10 GHz can create shallow penetration of energy and are therefore ideal for near-surface-based treatments. Microwave heating of skin causes molecular dipole rotation because of the high water content as well as sweat ducts and underlying tissues.[18,20] Furthermore, skin layers exhibit dielectric polarization when exposed to microwaves.[18,21] Skin layers are not as permeable to microwaves as much as to conductors.[22] Synovial joints and surrounding soft tissues have high fluid concentration and dielectric properties. Subsequently, an appropriate level of microwave power is needed to penetrate the joint and decrystallize embedded crystal aggregates formed in gouty tophi.

The Aslan Research Group recently described a technique known as the metal-assisted and microwave-accelerated decrystallization (MAMAD) technique, which is used to decrystallize crystals on the basis of the combined use of microwaves and gold nanoparticles (AuNPs) in solution.[23] In the MAMAD technique, kinetic energy of AuNPs suspended in a buffer solution (at physiological pH) can be significantly increased by microwave energy. Increased kinetic energy results in increased collisions between the AuNPs in solution and the target crystals are placed on a surface.[12,23] Subsequently, uric acid and other gout-related crystals on a surface can be decrystallized by the combined use of AuNPs and microwave heating, that is, the MAMAD technique.

In this study, we investigated the effect of microwave heating on a synthetic skin sample using a solid state, medical microwave source at 8 GHz. The power level of the microwave and the duration of the microwave heating were varied between 2 and 20 W and 0 and 120 s, respectively. Qualitative and quantitative assessment of skin damage was carried out using optical microscopy and real-time temperature measurements. Synthetic skin samples were used to simulate the real human skin for future potential applications of the MAMAD technique for the treatment of acute and chronic gout. We also investigated whether the size of a large crystal (L-alanine, a model crystal for tophi) placed under a synthetic skin sample can be reduced in the presence of AuNPs (20 nm) using the MAMAD technique. Finite-difference time-domain (FDTD) simulations were carried out to predict the extent of interactions of 8 GHz monomode microwave radiation with synthetic skin samples. In addition, change in temperature of synthetic skin samples at an initial temperature of 20 °C during 120 s of microwave heating was simulated and compared with that of experimental temperature measurements.

## RESULTS AND DISCUSSION

To establish a baseline for the quantification of damage to synthetic skin samples by medical microwaves, optical images of synthetic skin samples before their exposure to microwave heating were obtained at different temperatures (Figure S1, Supporting Information). The temperature range of synthetic skin samples was chosen to vary between physiological temperatures of 20 and 39 °C, which is based on the future potential application of the MAMAD technique in humans. Synthetic skin used in this study has a similar texture and consistency to the actual human skin tissue as well as a similar puncture pressure of 2 N/mm$^2$ as compared to 2.5 ± 0.3 N/mm$^2$ for human skin.[24] We note that toughness of the human skin depends on the structural collagen network embedded in the tissues, the density of collagen fibers, the location of the punctured skin (e.g., skin on the finger, back, or leg), and the tools used to puncture the skin (sharp or blunt). As each synthetic skin sample was prepared separately and a variation in the initial temperature of samples before their exposure to microwave results in a variation in the initial surface area of synthetic skin samples as evidenced by upper and lower views


DOI: 10.1021/acsomega.6b00233
ACS Omega 2016, 1, 744−754

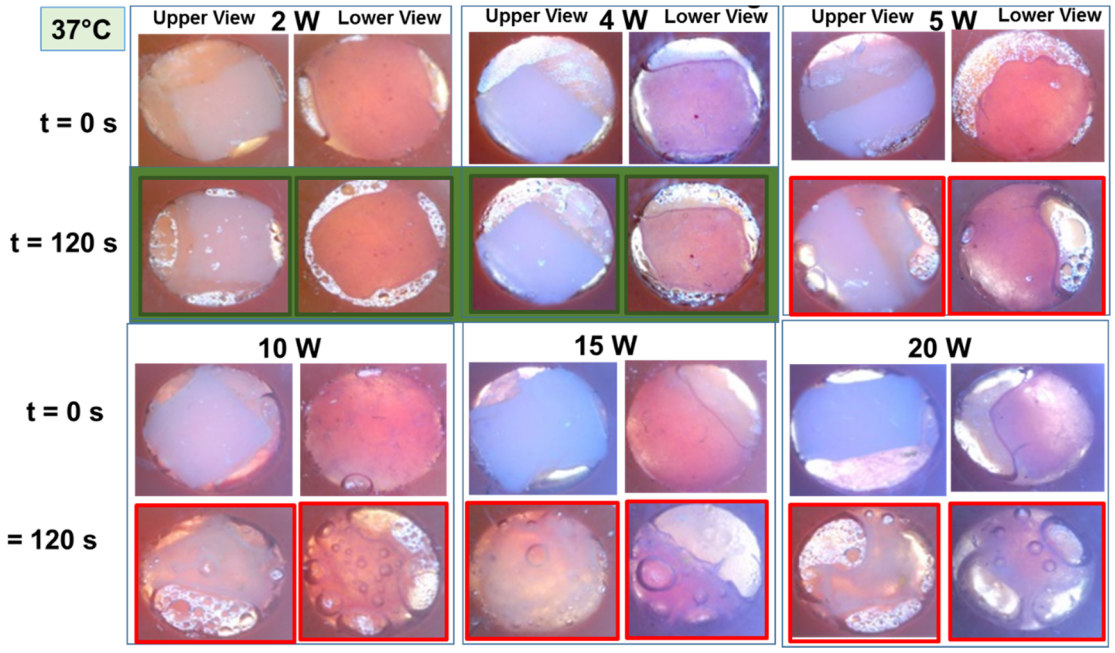


**Figure 2.** Qualitative assessment of skin damage via visual confirmation. Real-color pictures of synthetic skin samples at body temperature (assessed up to 120 s at initial temperature of 37 °C and $t$ = 0 s) before and after their exposure to 20 s intervals of microwave heating at 2, 4, 5, 10, 15, and 20 W. Green frames denote no tissue damage at 2 and 4 W. Red frames denote tissue damage after 120 s of microwave heating at 5, 10, 15, and 20 W.

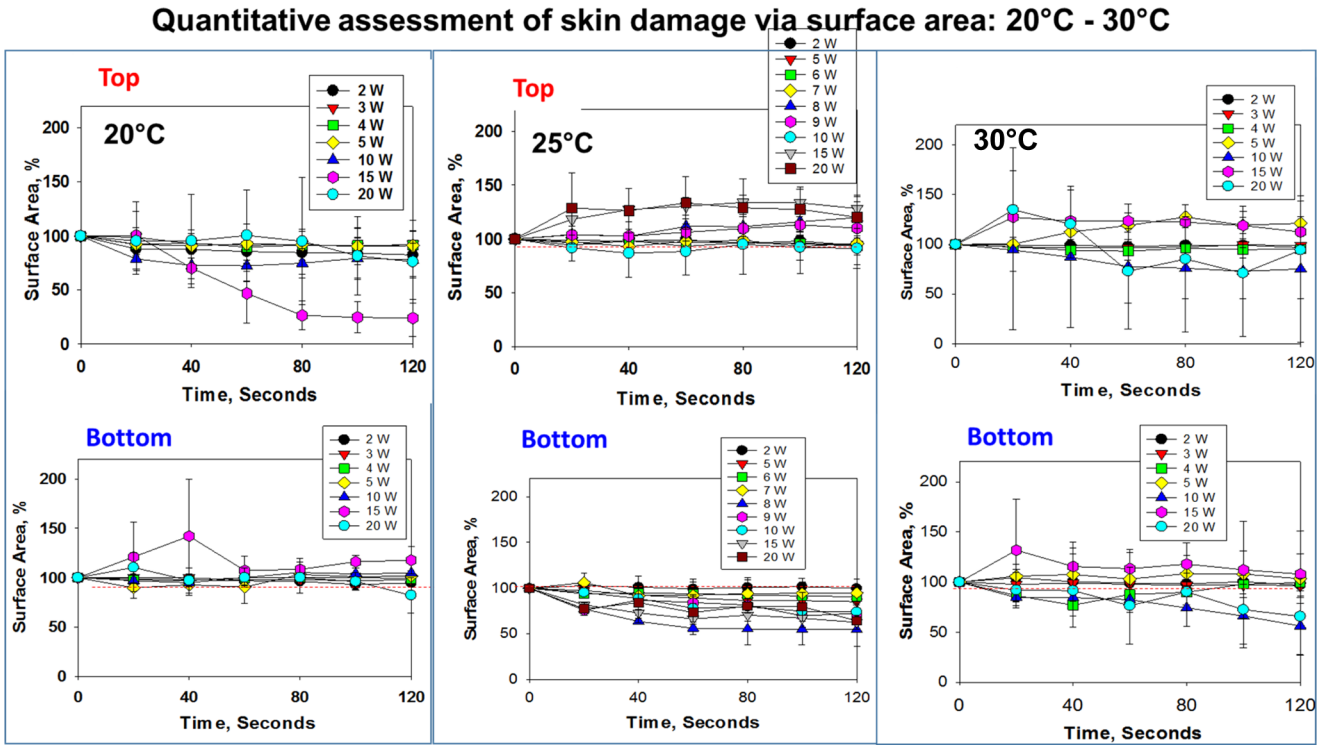


**Figure 3.** Reduction of surface area of the synthetic skin sample during microwave heating (2−20 W) up to 120 s. Initial temperature of the synthetic skin sample was adjusted to 20, 25, and 30 °C. An increase in surface area (in %) denotes the physical expansion of the synthetic skin sample and a decrease in the surface area indicates the physical reduction of the synthetic skin sample.

of these samples, pictures of all synthetic skin samples were taken in the beginning of the experiments (Figure S1).

Real-color pictures of synthetic skin samples at initial temperatures of 20−39 °C before and after their exposure to 20 s intervals of microwave heating (up to 120 s) using an 8 GHz, solid-state microwave source at 2−20 W are used for qualitative and quantitative assessment of skin damage and these results are given in Figures 1, 2, S2, and S10.

Our reasoning for the use of initial temperatures lower than the physiological temperature is to simulate conditions, where the potential application of medical microwaves on inflamed joints can be tolerated more comfortably by gout patients.



DOI: 10.1021/acsomega.6b00233
ACS Omega 2016, 1, 744−754

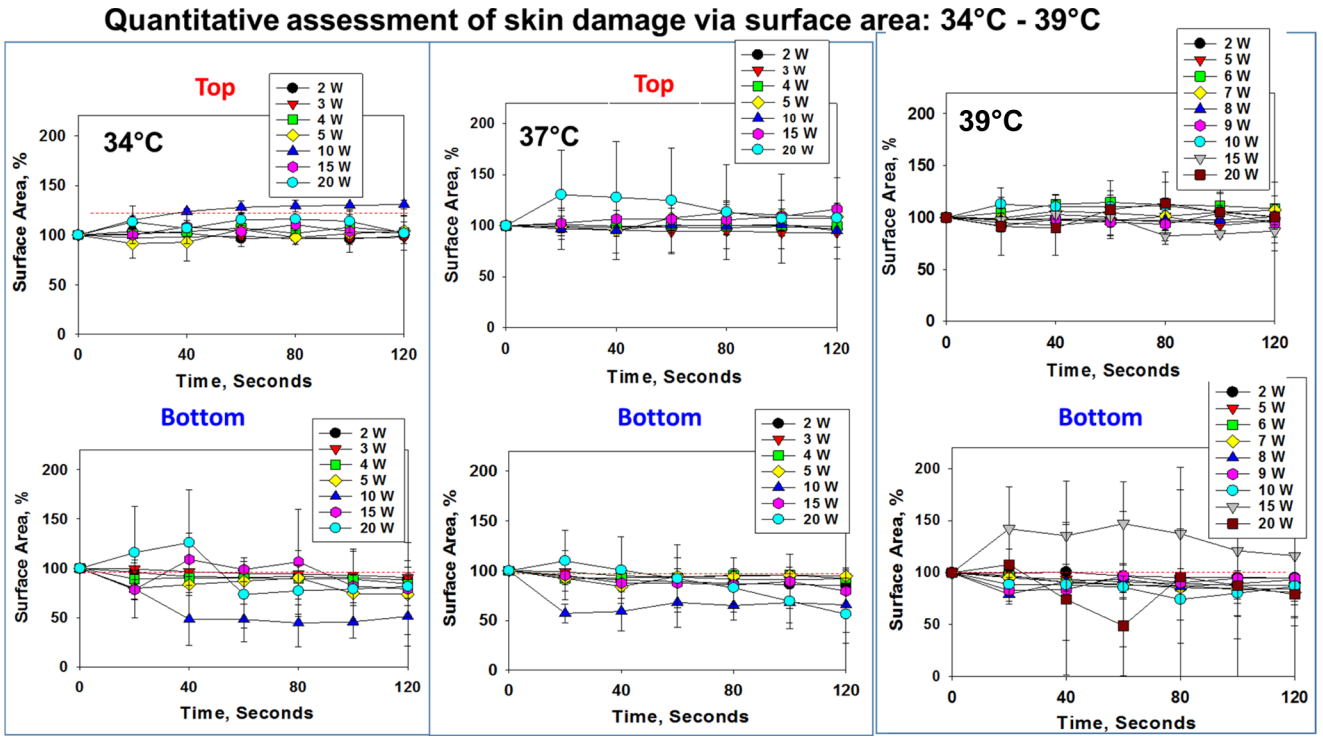


**Figure 4.** Reduction of surface area of the synthetic skin sample during microwave heating (2−20 W) up to 120 s. Initial temperature of the synthetic skin sample was adjusted to 34, 37, and 39 °C. An increase in surface area (in %) denotes the expansion of the synthetic skin sample and a decrease in the slope indicates the reduction of the synthetic skin sample.

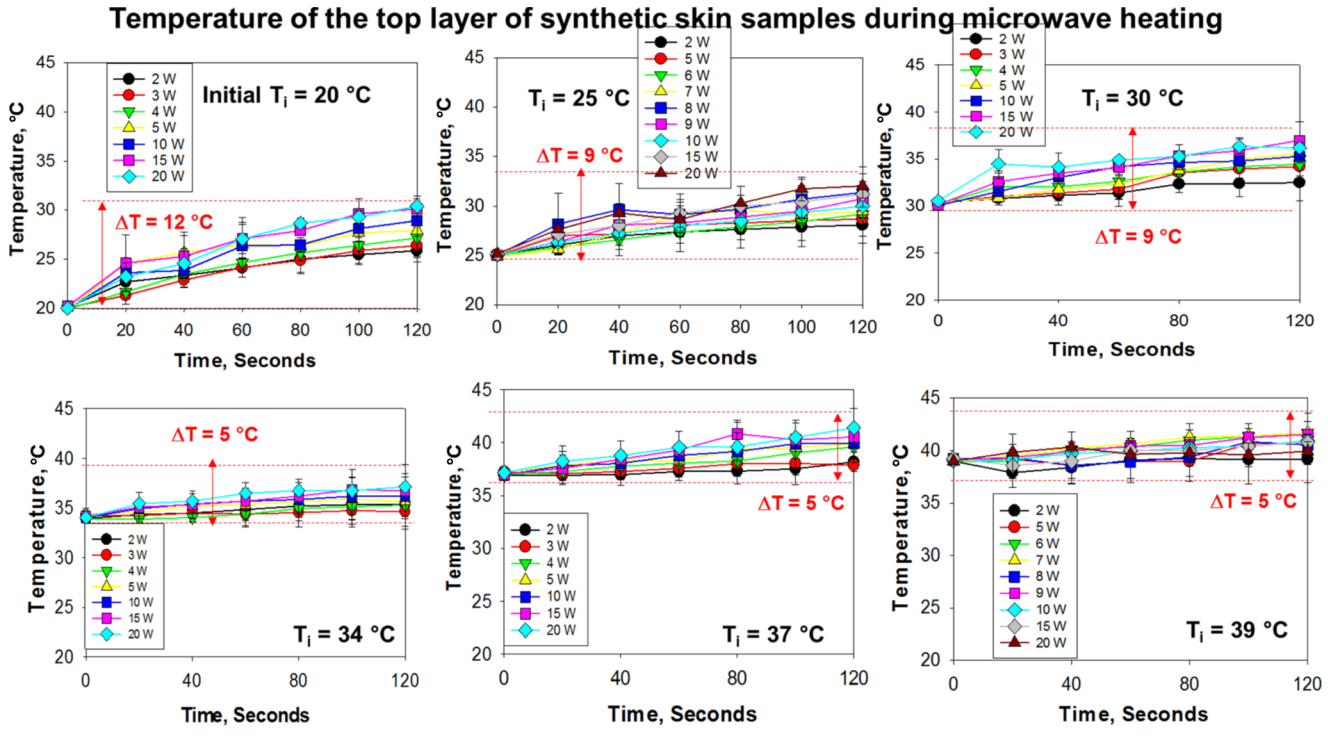


**Figure 5.** Change in temperature of the synthetic skin sample during microwave heating to assess potential changes in surface area (2−20 W) up to 120 s. Initial temperature of the synthetic skin sample was adjusted to 20, 25, 30, 34, 37, and 39 °C. Room temperature was ∼25 °C at the time of experiments.

Figure 1 shows the summary of the results for qualitative assessment of damage to synthetic skin samples kept at an initial temperature of 20 °C after 120 s of microwave heating at various microwave power levels (2−20 W).

Visual inspection of synthetic skin samples after 120 s of microwave heating at a microwave power range of 2−4 W shows a negligible change in the surface area of synthetic skin samples and water vapor bubbles form around the skin samples.



DOI: 10.1021/acsomega.6b00233
*ACS Omega* 2016, 1, 744−754

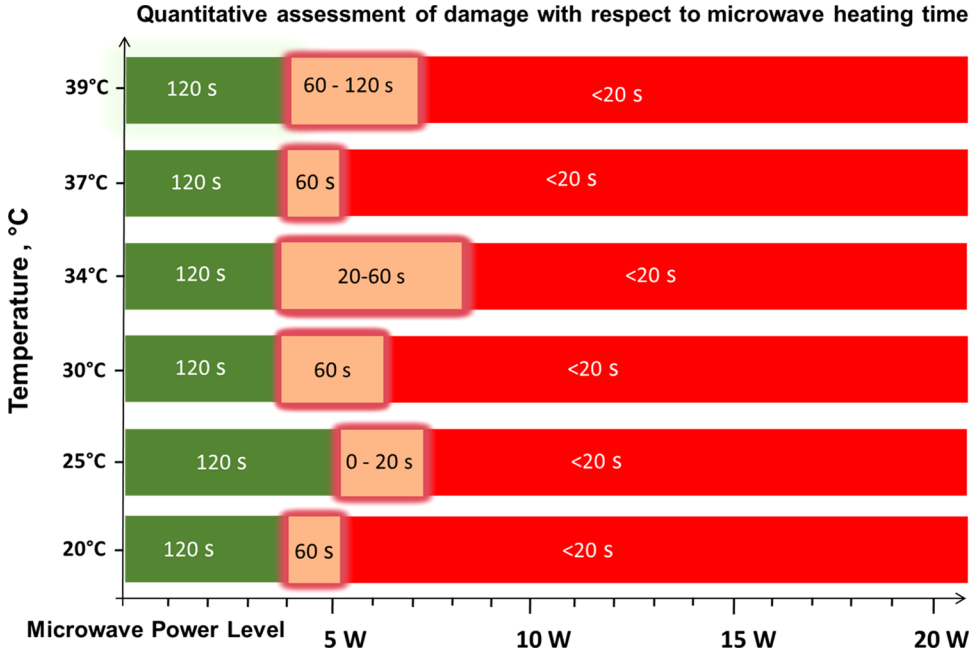


**Figure 6.** Quantitative assessment of skin damage with respect to microwave heating time. Green scale denotes the time and microwave power where no tissue damage was observed in the synthetic skin sample (note that the initial temperature of the synthetic skin sample was adjusted to the values given in *y* axis). "Glowing" orange scale is the "transition zone" where minor tissue damage was observed. Red scale denotes significant tissue damage. Time values indicate the duration of microwave heating where synthetic skin samples remain undamaged.

Further increase in the microwave power level to higher than 5 W resulted in a significant change in the surface area and formation of larger water vapor bubbles. In addition, these experiments were repeated with synthetic skin samples kept at different temperatures. For example, to simulate the physiological temperature conditions in humans, synthetic skin samples at 37 °C were exposed to 20 s intervals of microwave heating up to 120 s and the summary of these results are shown in Figure 2. Visual inspection of synthetic skin samples shows negligible skin damage for microwave power less than 4 W and significant damage at microwave power levels of higher than 5 W. Similar damage trends were also observed for the remainder of synthetic skin samples studied (Figures S2 and S5).

It is important to explain the choice of time interval of 20 s of microwave heating of the synthetic skin samples. Our previous[25−28] and ongoing studies involving solid-state[29] and conventional microwaves[30] for the decrystallization of organic and inorganic crystals[31] show that 20 s of microwave heating time is optimum in controlling the temperature changes in the medium with target crystals.[23] As our ultimate aim is to potentially employ the MAMAD technique for the decrystallization of gout-related crystals in humans, precise control over temperature change is critically important to minimize the damage to biological samples. In this regard, to investigate the extent of damage to synthetic skin samples during 20 s intervals of microwave heating, we have carried out a series of experiments by capturing real-color pictures of both sides of synthetic skin samples and measuring the temperature of the top layer of samples simultaneously (our experimental setup restricted our ability to measure the temperature of the bottom layer).

Real-color pictures of synthetic skin samples at initial temperatures of 20−39 °C before and after their exposure to 20 s intervals of microwave heating (up to 120 s) were used for the quantitative assessment of skin damage (Figures S6−S11). In this regard, the extent of change in the surface area of synthetic skin samples was calculated using real-color pictures and ImageJ software and results are shown in Figures 3 and 4. Upon exposure of synthetic skin samples at 20 °C to microwave heating at 2−10 W, the surface areas of the top and bottom layers of synthetic skin samples show no significant change. On the other hand, the surface area of synthetic skin samples at 20 °C appears to decrease significantly when the microwave power is increased to higher than 10 W. As the initial temperature of synthetic skin samples is increased to 25 and 30 °C, microwave heating of skin samples resulted in an increase (∼50%) in the surface area of the top layers of the samples. In addition, the surface area of the bottom layers of synthetic skin samples also shows greater variability during microwave heating (Figure 3). The observed changes can be explained by up to 12 °C increase in temperature of the samples because of microwave heating (Figure 5) and partially by experimental error (synthetic skin samples are relatively fragile when cut into small pieces and force is applied by the microwave applicator). It is also important to note that the evaporation of water within the layers of synthetic skin samples because of microwave heating contributes to the change in the surface area, where the evaporation of water generates air pockets around and throughout the samples (the sample holder is sealed and the escape of water vapor from the system is prevented). As the extent of air pockets in the system is unknown and is included in the overall calculation of the surface area, the standard deviation values significantly vary for synthetic skin samples with extensive water vapor formation after their exposure to microwave heating.

Figure 4 shows that the change in the surface area of the top layer of synthetic skin samples at 34−39 °C is significantly less (up to 20% change) during microwave heating as compared to that of synthetic skin samples kept at temperatures lower than 30 °C. This observation can be partially explained by a smaller


DOI: 10.1021/acsomega.6b00233
ACS Omega 2016, 1, 744−754

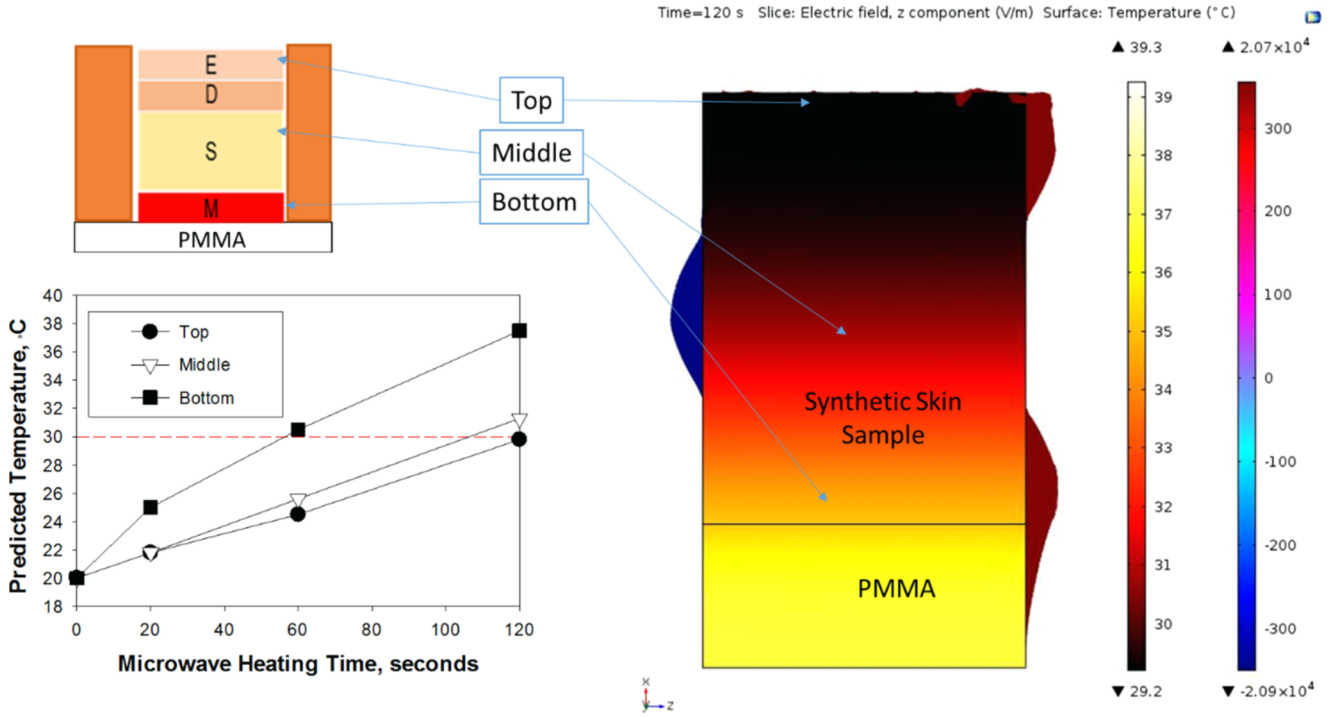


**Figure 7.** COMSOL simulations of temperature and electric field distributions for an 8 GHz microwave source in a waveguide with synthetic skin samples placed on between a cover slip and iCrystal plates. Microwave power input = 10 W, $t$ = 120 s.

increase in temperature (~4 °C) of the samples kept at 34−39 °C (Figure 5). However, the surface area of the bottom layer of synthetic skin samples at 34−39 °C varies up to 50% of its original value, which can be attributed to a greater extent to the evaporation of water within synthetic skin samples and the subsequent formation of vapor bubbles around and throughout the samples.

As the MAMAD technique involves the use of microwave heating, it is important to measure and control the temperature of synthetic skin samples to assess the potential contribution of the change in temperature of samples to damage. Figure 5 shows the change in temperature of synthetic skin samples kept at various initial temperatures during microwave heating (2−20 W). The largest change in temperature ($\Delta T$ = 5−12 °C) of synthetic skin samples after 120 s of microwave heating was observed for those kept at an initial temperature of 20 °C. As the initial temperature of synthetic skin samples was increased to 39 °C, the change in temperature was gradually decreased to the range of 1−5 °C. These observations can be explained by the multiple heat transfer events that occur during the microwave heating of synthetic skin samples. As the temperature of the room was 25 °C at the time of collection of the data presented here, initial temperature of synthetic skin samples at 20 °C is cooler than the room temperature and in an attempt to reach thermal equilibrium the samples absorb heat from the surroundings. Combined with the application of microwave heating to the samples for 120 s that provides an additional source of heating for the samples, the temperature of the samples was increased from 20 to ~32 °C in 120 s. The increase in temperature for synthetic skin samples already kept at 25 and 30 °C was up to the range of 2−9 °C, which in most part can be attributed to the microwave heating. On the other hand, when the initial temperature of synthetic skin samples (>34 °C) is significantly higher than room temperature (25 °C), the increase in temperature is up to the range of 1−5 °C. In this regard, as the initial temperature of synthetic skin samples is higher than room temperature, in an attempt to reach thermal equilibrium, the samples transfer heat to the surroundings (i.e., cooling). However, synthetic skin samples are exposed to microwave heating and the overall effect of both cooling and microwave heating is an increase in the temperature. These results imply that the initial temperatures of the samples and the surroundings play an important role in the overall temperature change of the samples: microwave heating (20 s intervals, 120 s total heating time) of synthetic skin samples results in up to 9 °C increase in temperature for samples kept at 25 °C, and an additional ~3 °C increase in temperature for samples kept at 20 °C and a decrease of ~3 °C for samples kept at >34 °C.

On the basis of the observations described above, quantitative assessment of skin damage with respect to microwave heating can be summarized in Figure 6. According to our results, synthetic skin samples kept at an initial temperature range of 20−39 °C can safely be exposed up to 4 W of microwave heating (8 GHz) for up to 120 s without structural damage (green zone, Figure 6). Synthetic skin samples can also tolerate exposure to increased microwave power up to 7 W for additional 20−120 s, where a 50% loss of physical stability can be expected (orange zone, Figure 6). However, because of the loss of physical stability of synthetic skin samples, the use of microwave power higher than 7 W is not recommended (red zone).

To investigate the extent of interactions of monomode microwaves at 8 GHz with synthetic skin samples placed in iCrystal plates, two predictive simulation tools based on FDTD calculations of temperature and electric field distributions were employed (Figures 7 and S13). Figure 7 shows the temperature and electric field distributions across the virtual model generated for synthetic skin sample and the iCrystal plate predicted by COMSOL software. Theoretical calculations


DOI: 10.1021/acsomega.6b00233
ACS Omega 2016, 1, 744−754

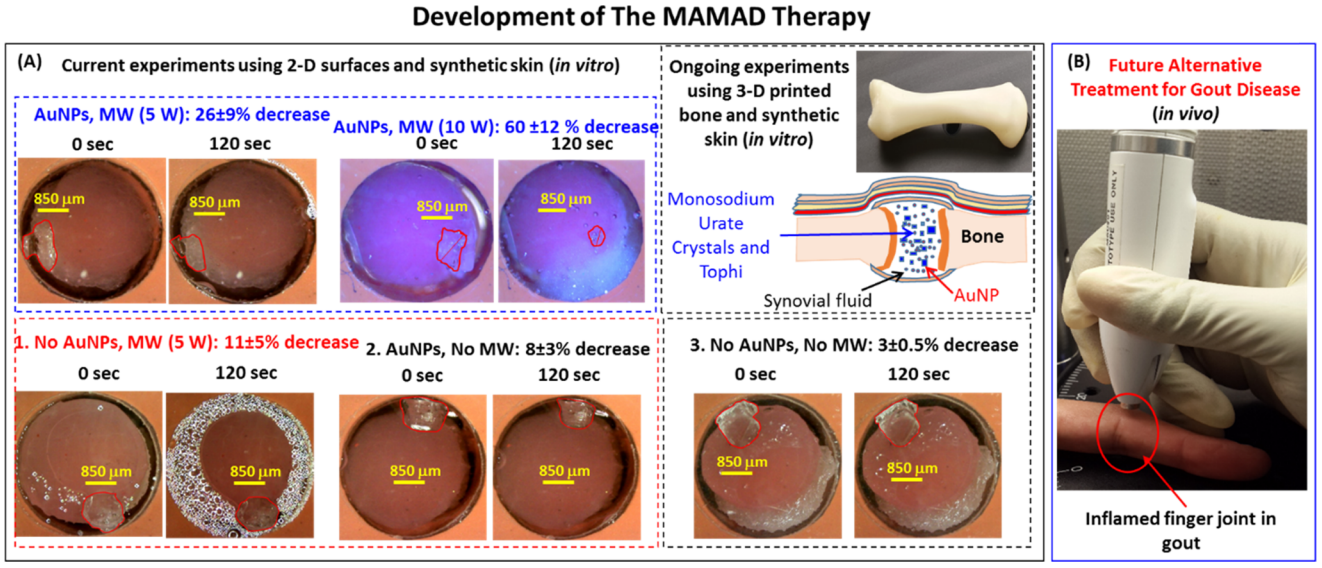


**Figure 8.** Potential future application of the MAMAD therapy. (A) The proof-of-principle demonstration of the MAMAD technique for the potential treatment of advanced gout using L-alanine as model tophi, synthetic skin on 2-D surfaces and three-dimensional (3-D) printed bones (in vitro). The size of the L-alanine crystals was reduced using the MAMAD technique with AuNPs. Synthetic skin samples were kept at 37 °C. (B) Potential future application of the MAMAD technique for the treatment of gout at various stages of the diseases by medical professionals.

predict a variation in the temperature throughout the synthetic skin sample (Figure 7): for microwave heating at 10 W, the temperature of the top portion of the synthetic skin sample is predicted to increase from an initial temperature of 20 to 30 °C in 120 s, which is comparable to that of the actual temperature measurement provided in Figure 5. The temperature of the middle portion of the synthetic skin sample is predicted to increase similar to that of the top portion; however, the temperature of the bottom portion of the synthetic skin sample is predicted to increase from an initial temperature of 20 to 38 °C in 120 s, which can be attributed to the higher temperature of the iCrystal plate. As microwave heating progresses, poly(methyl methacrylate) (PMMA) (bottom part of the iCrystal plate) heats up more quickly as compared to synthetic skin sample and subsequently heat transfer from PMMA to synthetic skin sample results in an increase in the temperature of the bottom portion of the synthetic skin sample that accounts for the predicted variations in the temperature throughout synthetic skin samples.

It is important to note that the initial temperature of the system was set to 20 °C and additional heat transfer from the surroundings (room temperature = 25 °C) to the system was not considered in these predictive calculations. As the current simulation model created in COMSOL is not capable of calculating all possible heat transfer events that occur during microwave heating of synthetic skin samples on the iCrystal plates, no additional calculations were carried out for other experimental conditions reported in this study. Further studies are underway and will be reported in due course.

In addition to COMSOL simulations, an open-source FDTD-based simulation tool to predict the extent of absorption of electromagnetic energy by synthetic skin samples was used. In this regard, transmission (T) and reflection (R) spectra were recorded at a single frequency of 8 GHz by placing detectors at the bottom and top parts of the simulation cell, respectively (Figure S13). The absorption (A) percentage was calculated with A = 1 − (T + R) by using the simulated values. Simulation results show that the electric field is predicted to propagate through synthetic skin samples, where the monomode microwave radiation intensity is significantly reduced by the samples. The transmission and reflection spectra simulations showed that the three-layer structure (synthetic skin, cover slip, and the iCrystal plate) absorbed ∼92.2% of the 8 GHz monomode microwave radiation, where ∼5.2% was transmitted and ∼2.6% was reflected back into the source. Separate simulations showed that the cover slip and the iCrystal plates had negligible absorption under 8 GHz microwave radiation. These predictions imply that the synthetic skin sample can be effectively heated within 2 min, which is corroborated by experimental temperature measurements.

Figure 8A shows the proof-of-principle demonstration of the MAMAD technique for decrystallization of L-alanine (model tophi for advanced gout) through synthetic skin sample in the presence of AuNPs. In this regard, L-alanine crystals and a solution of AuNPs (20 nm in diameter) were placed at the bottom of an iCrystal plate and covered with synthetic skin sample and exposed to 5 and 10 W of microwave heating for up to 120 s with 20 s intervals. We note that the choice of 10 W is on the basis of the following thought process: it is hypothesized that the presence of AuNPs near the synthetic skin sample can extend the durability of the synthetic skin sample to microwave heating above the <7 W microwave power threshold for minimal damage to skin. In this regard, to demonstrate the significance of combined use of microwaves and AuNPs, three control experiments were carried out: (1) control experiment 1 = solution of AuNPs is omitted (no AuNP) and 5 W microwave heating is applied, (2) control experiment 2 = AuNP present, no microwave heating, and (3) control experiment 3 = no AuNP, no microwave heating. In the first control experiment, where the solution of AuNPs is omitted, microwave heating of L-alanine crystals resulted in 11% reduction in size. This observation implies that microwave-accelerated decrystallization of crystals can be achieved. Moreover, when microwave heating is omitted and only AuNPs are used (metal-assisted decrystallization), the size of L-alanine crystals can be reduced up to 8%. In addition, the


DOI: 10.1021/acsomega.6b00233
ACS Omega 2016, 1, 744−754

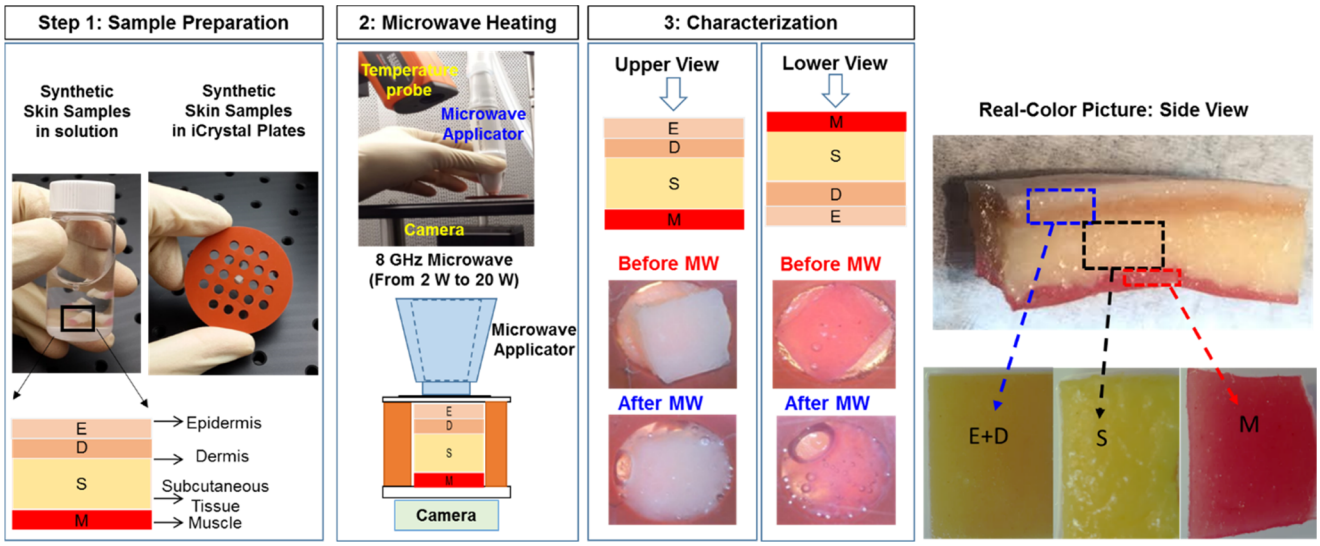


**Figure 9.** Schematic illustration of our experimental process. Synthetic skin samples (at initial temperature range 20−39 °C) are subjected to specified microwave power levels. Real-color pictures of synthetic skin samples (bottom and top sides) are captured to visually and quantitatively assess the damage because of microwave energy. Real-color, high-resolution picture of the synthetic skin construct and its individual components are shown.

contribution of dissolution of L-alanine crystals at room temperature without AuNPs was found to be 3% (control experiment 3). When the MAMAD technique (i.e., combined use of AuNPs and microwave heating) is applied, the size of the L-alanine crystal was reduced 26 and 60% in the samples with AuNPs exposed to 5 and 10 W of microwave heating, respectively. An increase in microwave power from 5 to 10 W clearly increases the extent of decrystallization of L-alanine. A closer inspection of synthetic skin samples exposed to 10 W of microwave power in the presence of AuNPs reveals negligible damage, as opposed to significant skin damage observed without AuNPs as shown in Figure 7 and as described earlier in the text. To investigate the effect of the presence of AuNPs near synthetic samples during microwave heating, the temperature of synthetic skin samples kept at 20 °C was monitored in the absence and presence of AuNPs and L-alanine crystals during 120 s of microwave heating at 5 and 10 W (Figure S12). These measurements reveal that the temperature of the synthetic skin sample with AuNPs (labeled as 10 W with Au) remained ∼1 °C cooler than that of the synthetic skin sample without AuNPs, which can directly be attributed to the presence of AuNPs and L-alanine crystals and can explain the observed negligible damage to synthetic skin sample exposed to 10 W of microwave power.

On the basis of these initial observations, our laboratory is currently working on furthering the applicability of the MAMAD technique by additional experiments using AuNPs of various sizes, where gout-related crystals are decrystallized in exact polymeric replicas of human bones prepared using a commercially available 3-D printer and synthetic skin (Figure 8A). These observations imply that the MAMAD technique can be potentially used for decrystallization of crystalline materials related to gout disease through human skin in the future (Figure 8B).

## MATERIALS AND METHODS

**Materials and Instrumentation.** Synthetic skin was purchased from SynDaver Labs (Tampa, FL). PMMA disks (diameter = 5 cm) were purchased from McMaster-Carr (Elmhurst, IL) and 21-well silicone isolator (depth = 2.0 mm, capacity = 30 $\mu$L, diameter = 4.5 mm) were purchased from Grace Bio-labs (Bend, OR). The antialgae solution was purchased from Clorox (Lawrenceville, GA) and cyanoacrylate was purchased from Gorilla (Cincinnati, OH). L-Alanine powder was purchased from Sigma-Aldrich. An incubator (Model 10-140) with a photo-optic lamp was purchased from Osram (Munich, Germany).

A compact medical microwave (ISYS800, 20 W) with an 8 GHz microwave generator was obtained from Emblation (Scotland, UK). A digital microscope camera UM12 5 MP USB was purchased from ViTiny (Taylors, SC) and a Klein Tools IR1000 12:1 Infrared Thermometer was purchased from Kline Tools (Lincolnshire, IL). Deionized water was obtained using a Millipore Direct-Q 3 UV apparatus maintained at resistivity = 18.2 MΩ cm. 20 nm AuNPs (catalog number 741965: $7.2 \times 10^{11}$ particles/mL) were purchased from Sigma-Aldrich (Milwaukee, WI) and as used without further modification.

**Preparation of the Synthetic Skin.** Synthetic skin used for experiments represented the skin of a Caucasian adult and consisted of bonded and nonbonded synthetic polymers, characteristic of the epidermis, dermis, subcutaneous, and muscle layers of the skin (Figure 9). The bonded epidermis and dermis layers' tissue plate samples were measured to be 2 mm thick. The subcutaneous fat layer and the muscle layer tissue plates were nonbonded layers; these sections were measured to be 5 and 2 mm thick, respectively. The subcutaneous layers were adjusted to 2 mm for a total synthetic skin thickness of 6 mm. Synthetic skin (as purchased) is 2 mm thicker than human skin tissue at actual tophi site, which is approximately 2−4 mm in thickness.

The thickness of the synthetic skin was adjusted with the use of a surgical knife until it measured 1.5−2 mm and was made comparable to that of human skin layers. Bonding of the three synthetic skin tissue plates was done with the use of a cyanoacrylate glue to form a model that represented all skin components. Synthetic skin samples were sectioned into 4.5 mm (width) × 6 mm (height) pieces and immersed into an


DOI: 10.1021/acsomega.6b00233
ACS Omega 2016, 1, 744−754

antialgae solution. Synthetic skin samples were then stored in sealed 20 mL scintillation vials and refrigerated at 4 °C to prevent contamination and to maintain the integrity of the synthetic skin samples. Subsequently, synthetic skin samples were processed under a laminar flow hood to prevent contamination and stored in an incubator before use. An ice bath and an incubator were used to adjust the initial temperature of synthetic skin samples between the range of 20 and 39 °C.

An 8 GHz compact microwave generator with a maximum variable power of 20 W was used to test the physical stability of synthetic skin samples. The wavelength of 8 GHz microwaves is ∼3.75 cm and microwaves are expected to completely penetrate (minus the absorption of microwaves by the skin) the depth of synthetic skin samples used in this study. Upon completion of the test on synthetic skin, the MAMAD technique was applied with the use of AuNPs and L-alanine as a model crystal. All samples were analyzed under a digital microscope. Further experimental details are provided in the following sections.

**Microwave Heating of the Synthetic Skin.** Synthetic skin samples were placed in the sample holders of an iCrystal plate (Figure 9, each well is 4.5 mm in diameter and 6 mm in depth) and monitored with a microscope during microwave heating. A glass cover slip was placed over the synthetic skin during microwave heating. The real-color pictures of synthetic skin samples (bottom and top views) were captured before and after microwave heating. Synthetic skin samples were exposed to microwaves (2−20 W using the following increments: 2, 4, 5, 10, 15, and 20 W) for 20 s and up to 120 s. The initial temperature of the synthetic skin samples ranged from 20 to 39 °C (20, 25, 30, 34, 37, and 39 °C) to simulate future potential applications of the MAMAD technique in humans. The captured real-color pictures of synthetic skin samples (top and bottom surfaces) were used to quantify and assess the progression of the microwave-induced damage to synthetic skin samples. An infrared thermometer was used to measure the temperature of the top layer of synthetic skin that was exposed directly to the microwave heating. As microwaves were applied, the bottom of the sample was monitored with another digital video camera. The digital images of synthetic skin samples were examined for changes observable with naked eye. In addition, in control experiments, synthetic skin samples were kept at temperatures ranging from 20 to 39 °C without microwave heating. Changes in the surface area of all synthetic skin samples were quantified using ImageJ software.

**Decrystallization of L-Alanine Using the MAMAD Technique.** L-Alanine crystals (a surface area of approximately 4 $mm^2$) were used as a model for large crystal mass (tophi) associated with gout. Synthetic skin samples were placed in the well of an iCrystal plate with L-alanine crystals and solution of 20 nm AuNPs. In control experiments, AuNPs were omitted from the samples as described above. Microwave power levels for the decrystallization experiments were chosen on the basis of the extent of damage sustained by synthetic skin samples and the range of increase in temperature (up to 12 °C but less than 41 °C) as observed from the experiments described in the previous section. Both samples were exposed to 8 GHz microwave power at 7 W for a total of 120 s and monitored with an optical microscope. All experiments in this study were repeated a minimum of three times and the average of the data with standard deviation was reported.

**COMSOL Theoretical Simulations.** COMSOL Multiphysics software (version 5.2) includes an in-built microwave heating model for a conventional microwave oven, which was modified to simulate electric field and temperature distributions of 8 GHz (monomode microwave source) across a model structure generated for synthetic skin and an iCrystal plate. Synthetic skin (surroundings: air and silicone isolators) and iCrystal plates were used as a target sample for microwave heating at 10 W. We note one can study any microwave power in simulations. We have chosen 10 W microwave power as an example. Calculations related to microwave heating are described by Maxwell's equations and have been previously published.[32−34] A frequency transient study with a time-dependent solver (20 s steps up to 120 s) was conducted for the whole system rather than for a symmetric half. The FDTD method was used in computation of equations in COMSOL Multiphysics software. Heat transfer study module of COMSOL Multiphysics software is also used to predict the heat distribution across wells during microwave heating steps.

**FDTD Studies.** Additional FDTD simulations were performed to determine the percentage of microwave absorption by the skin sample. Massachusetts Institute of Technology's (MIT) open-source MIT Electromagnetic Equation Propagation (MEEP) FDTD software[35] was utilized for the two-dimensional (2-D) transmission, reflection, and electric field visualization simulations. In the electric field visualization simulations, a virtual three-layer structure (4.5 mm wide) composed of a synthetic skin (6 mm thick), a 100 $\mu$m thick borosilicate glass cover slip, and a 2 mm thick iCrystal plate, where the skin was modeled according to dielectric properties of human skin.[36] In addition, an 8 GHz monomode microwave radiation was modeled as a fixed frequency continuous source located on the top part of the simulation cell. The simulation cell was padded with 1 mm thick perfectly matched absorbing layers (i.e., silicone isolators). In the experiments, the microwave source is directed to the skin sample via a flexible waveguide. Thus, the 8 GHz (full wavelength = 3.75 cm) source was placed in a 4.5 mm wide waveguide with a dielectric constant value of 17.3. The corresponding wavelength of the microwave radiation in the waveguide is 9 mm, which ensures monomode propagation throughout the constructed structure.

## CONCLUSIONS

The effect of microwave heating of a synthetic skin sample using a solid-state medical microwave source (8 GHz and 2−20 W power) was investigated. Synthetic skin samples kept at 20−39 °C were heated at 20 s intervals up to 120 s. Qualitative assessment of skin damage carried out using optical microscopy showed that microwave heating of synthetic skin sample causes negligible damage for microwave power up to 7 W and significant damage at microwave power >7 W, on the basis of the summary provided in Figure 7. Optical microscope images of synthetic skin samples were also processed using ImageJ software to calculate the change in the surface area during microwave heating for the quantitative assessment of skin damage. The extent of damage to synthetic skin samples was negligible for microwave power <7 W and more extensive damage (>50%) to synthetic skin samples occurred when exposed to >7 W microwave heating. The observed damage to synthetic skin samples was attributed to the evaporation of water within the layers of synthetic skin samples because of microwave heating, which contributes to the change in the surface area because of the generated air pockets around and throughout the samples. In addition, the initial temperature of



DOI: 10.1021/acsomega.6b00233
ACS Omega 2016, 1, 744−754

synthetic skin samples before exposure to microwave heating was found to affect the extent of change in temperature of the skin samples during microwave heating. Although a 12 °C increase in temperature for synthetic skin samples kept at an initial temperature of 20 °C was observed, the change in temperature was significantly less (5 °C) for synthetic skin samples kept at higher initial temperatures >34 °C after 120 s of microwave heating. The proof of principle of the decrystallization of L-alanine crystals (a model crystal for tophi) through synthetic skin samples using the MAMAD technique was also demonstrated. Using the MAMAD technique, the size of L-alanine crystals placed under a synthetic skin sample can be reduced up to 60%, which can be directly attributed to the combined use of AuNPs and microwave heating. Theoretical calculations of electric field distributions of a monomode microwave source at 8 GHz show that electric field is predicted to propagate through synthetic skin samples and monomode microwave radiation intensity is significantly reduced by the structure.

## ■ ASSOCIATED CONTENT

### Supporting Information

The Supporting Information is available free of charge on the ACS Publications website at DOI: 10.1021/acsomega.6b00233.

Additional information related to optical images of synthetic skin samples before, during, and after microwave heating not shown in the main text is provided (PDF)

## ■ AUTHOR INFORMATION


### Corresponding Author

*E-mail: Kadir.Aslan@morgan.edu. Tel: 1 443 885 4257.


### Notes

The authors declare no competing financial interest.

## ■ ACKNOWLEDGMENTS

Research reported in this publication was partially supported by the National Institute of General Medical Sciences of the National Institutes of Health under Award Number UL1GM118973. The content is solely the responsibility of the authors and does not necessarily represent the official views of the National Institutes of Health.

## ■ REFERENCES


(1) Saccomano, S. J.; Ferrara, L. R. Treatment and prevention of gout. *Nurse Pract.* **2015**, *40*, 24−30 quiz 30-1..

(2) Desideri, G.; Castaldo, G.; Lombardi, A.; Mussap, M.; Testa, A.; Pontremoli, R.; Punzi, L.; Borghi, C. Is it time to revise the normal range of serum uric acid levels? *Eur. Rev. Med. Pharmacol. Sci.* **2014**, *18*, 1295−1306.

(3) Desideri, G.; Puig, J.; Richette, P. The management of hyperuricemia with urate deposition. *Curr. Med. Res. Opin.* **2015**, *31*, 27−32.

(4) Lockyer, S.; Stanner, S. Diet and gout−what is the role of purines? *Nutr. Bull.* **2016**, *41*, 155−166.

(5) Raina, S.; Raina, R. K.; Raina, S. K. Hyperuricemia: A risk factor beyond gout. *J. Obes. Metab. Res.* **2015**, *2*, 228.

(6) Schumacher, H. R. Pathology of the synovial membrane in gout. Light and electron microscopic studies. Interpretation of crystals in electron micrographs. *Arthritis Rheum.* **1975**, *18*, 771−82.

(7) Harris, M. D.; Siegel, L. B.; Alloway, J. A. Gout and hyperuricemia. *Am. Fam. Physician* **1999**, *59*, 925−34.

(8) Schlesinger, N. Management of acute and chronic gouty arthritis: present state-of-the-art. *Drugs* **2004**, *64*, 2399−416.

(9) Kim, K. Y.; Ralph Schumacher, H.; Hunsche, E.; Wertheimer, A. I.; Kong, S. X. A literature review of the epidemiology and treatment of acute gout. *Clin. Ther.* **2003**, *25*, 1593−617.

(10) Star, V. L.; Hochberg, M. C. Prevention and management of gout. *Drugs* **1993**, *45*, 212−22.

(11) Lee, S.-S.; Sun, I.-F.; Lu, Y.-M.; Chang, K.-P.; Lai, C.-S.; Lin, S.-D. Surgical treatment of the chronic tophaceous deformity in upper extremities−the shaving technique. *J. Plast. Reconstr. Aesthetic Surg.* **2009**, *62*, 669−674.

(12) Ettinoffe, Y. S.; Kioko, B. M.; Gordon, B. I.; Thompson, N. A.; Adebiyi, M.; Mauge-Lewis, K.; Ogundolie, T. O.; Bonyi, E.; Mohammed, M.; Aslan, K. Metal-Assisted and Microwave-Accelerated Decrystallization. *Nano Biomed. Eng.* **2015**, *7*, 139−149.

(13) Kumar, S.; Gow, P. A survey of indications, results and complications of surgery for tophaceous gout. *N. Z. Med. J.* **2002**, *115*, U109.

(14) Ertug, E.; Güzel, V. B.; Takka, S. Surgical management of tophaceous gout in the hand. *Arch. Orthop. Trauma Surg.* **2000**, *120*, 482−483.

(15) Wakim, K. G.; Herrick, J. F.; et al. Therapeutic possibilities of microwaves; experimental and clinical investigation. *J. Am. Med. Assoc.* **1949**, *139*, 989−93.

(16) Yadava, R. L. In *RF/microwaves in Bio-medical Applications*, Proceedings of the 8th International Conference on Electromagnetic Interference and Compatibility 2003 (INCEMIC 2003); IEEE, Dec 18−19, 2003; pp 81−85.

(17) Vrba, J.; Lapes, M. In *Medical Applications of Microwaves*, Proceedings of SPIE 5445, Microwave and Optical Technology 2003; International Society for Optics and Photonics, April 7, 2004; pp 392−397.

(18) Grant, J. P.; Clarke, R. N.; Symm, G. T.; Spyrou, N. M. In vivo dielectric properties of human skin from 50 MHz to 2.0 GHz. *Phys. Med. Biol.* **1988**, *33*, 607−12.

(19) Tamyis, N. M.; Ghodgaonkar, D. K.; Taib, M. N.; Wui, W. T. Dielectric properties of human skin in vivo in the frequency range 20−38 GHz for 42 Healthy volunteers, *Proceedings of the 28th URSI General Assembly*, New Delhi, 2005.

(20) Gabriel, C. *Compilation of the Dielectric Properties of Body Tissues at RF and Microwave Frequencies*; Accession Number: ADA309764, DTIC Document; King's College London: United Kingdom, 1996.

(21) Foster, K. R.; Schwan, H. P. Dielectric properties of tissues. *Handbook of Biological Effects of Electromagnetic Fields*; CRC Press, 1995; Vol. 2, pp 25−102.

(22) Kaatze, U. Techniques for measuring the microwave dielectric properties of materials. *Metrologia* **2010**, *47*, S91.

(23) Kioko, B.; Ogundolie, T.; Adebiyi, M.; Ettinoffe, Y.; Rhodes, C.; Gordon, B.; Thompson, N.; Mohammed, M.; Abel, B.; Aslan, K. Decrystallization of Uric Acid Crystals in Synovial Fluid Using Gold Colloids and Microwave Heating. *Nano Biomed. Eng.* **2014**, *6*, 104−110.

(24) Shergold, O. A.; Fleck, N. A. Experimental investigation into the deep penetration of soft solids by sharp and blunt punches, with application to the piercing of skin. *J. Biomech. Eng.* **2005**, *127*, 838−848.

(25) Mauge-Lewis, K.; Mojibola, A.; Aslan, K. Crystallization of lysozyme using metal-assisted and microwave-accelerated evaporative crystallization. *Abstracts of Papers of the American Chemical Society*; American Chemical Society: Washington, DC, 2014; Vol. 247.

(26) Mauge-Lewis, K.; Mojibola, A.; Toth, E. A.; Mohammed, M.; Seifu, D.; Aslan, K. Metal-Assisted and Microwave-Accelerated Evaporative Crystallization: Proof-of-Principle Application to Proteins. *Cryst. Growth Des.* **2015**, *15*, 3212−3219.

(27) Mohammed, M.; Aslan, K. Design and application of novel PMMA platform for microwave-accelerated bioassays. *Abstracts of Papers of the American Chemical Society*; American Chemical Society: Washington, DC, 2014; Vol. 247.




DOI: 10.1021/acsomega.6b00233
*ACS Omega* 2016, 1, 744−754

(28) Mojibola, A.; Dongmo-Momo, G.; Mohammed, M.; Aslan, K. Crystal Engineering of L-Alanine with L-Leucine Additive using Metal-Assisted and Microwave-Accelerated Evaporative Crystallization. *Cryst. Growth Des.* **2014**, *14*, 2494−2501.
(29) Mauge-Lewis, K.; Gordon, B.; Syed, F.; Syed, S.; Bonyi, E.; Mohamed, M.; Toth, E. A.; Seifu, D.; Aslan, K. Crystallization of Lysozyme on Metal Surfaces Using a Monomode Microwave System. *Nano Biomed. Eng.* **2016**, *8*, 60−71.
(30) Mohammed, M.; Syed, M. F.; Aslan, K. Microwave-accelerated bioassay technique for rapid and quantitative detection of biological and environmental samples. *Biosens. Bioelectron.* **2016**, *75*, 420−6.
(31) Kioko, B.; Ogundolie, T.; Adebiyi, M.; Ettinoffee, Y.; Rhodes, C.; Gordon, B.; Thompson, N.; Mohammed, M.; Abel, B.; Aslan, K. De-crystallization of Uric Acid Crystals in Synovial Fluid Using Gold Colloids and Microwave Heating. *Nano Biomed. Eng.* **2014**, *6*, 104−110.
(32) Sakai, N.; Mao, W.; Koshima, Y.; Watanabe, M. A method for developing model food system in microwave heating studies. *J. Food Eng.* **2005**, *66*, 525−531.
(33) Vadivambal, R.; Jayas, D. S. Non-uniform Temperature Distribution During Microwave Heating of Food Materials—A Review. *Food Bioprocess Technol.* **2010**, *3*, 161−171.
(34) Knoerzer, K.; Regier, M.; Schubert, H. A computational model for calculating temperature distributions in microwave food applications. *Innovative Food Sci. Emerging Technol.* **2008**, *9*, 374−384.
(35) Oskooi, A. F.; Roundy, D.; Ibanescu, M.; Bermel, P.; Joannopoulos, J. D.; Johnson, S. G. Meep: A flexible free-software package for electromagnetic simulations by the FDTD method. *Comput. Phys. Commun.* **2010**, *181*, 687−702.
(36) Gabriel, S.; Lau, R. W.; Gabriel, C. The dielectric properties of biological tissues: II. Measurements in the frequency range 10 Hz to 20 GHz. *Phys. Med. Biol.* **1996**, *41*, 2251.



DOI: 10.1021/acsomega.6b00233
*ACS Omega* 2016, 1, 744−754